J Mater Sci: Mater Med (2010) 21:787–795
DOI 10.1007/s10856-009-3869-z

Using small angle X-ray scattering to investigate the variation in composition across a graduated region within an intervertebral disc prosthesis

J. H. Gwynne · R. E. Cameron

Received: 20 August 2009 / Accepted: 31 August 2009 / Published online: 16 September 2009

Abstract The *CAdisc-L* is a polycarbonate urethane lumbar intervertebral disc prosthesis that aims to replicate the mechanical properties of a natural disc as closely as possible. In this work, Small Angle X-ray Scattering (SAXS) was used to investigate the variation in composition across prototype disc samples containing annulus and nucleus regions separated by a graduated region. An empirical data analysis method was developed involving the calculation of intensity ratios, since the SAXS data did not readily fit any of the standard analysis models. Calibration samples were used to quantify the variation in SAXS response with composition and a linescan method was employed to ascertain the change in composition across discs manufactured with different graduated region volumes. The graduated region width increases with the volume incorporated into it during manufacture, as expected, but the properties do not vary linearly across the graduated regions. The method developed during this work can be adapted for use with any series of polymer samples that shows a systematic variation in SAXS behaviour with composition.

1 Introduction

1.1 Intervertebral discs and disc prostheses

It is widely accepted that the degeneration of the intervertebral discs of the lumbar spine is a major cause of lower back pain [1]. Fortunately, most people respond well to non-operative treatments, but if surgery is required the traditional method used is spinal fusion, which involves the fusion of the vertebrae on either side of the affected disc [2]. Although many patients experience a satisfactory reduction in pain, fusion results in restricted motion and reduced spinal flexibility. Adjacent spinal levels compensate for the reduction in motion and compliance at fused joints, resulting in increased stresses on discs at levels adjacent to the fused disc. A patient who has disc degeneration is likely to have a predisposition to this disease at other levels, but the increased stresses due to fusion are likely to increase the rate at which their degeneration occurs [3].

These limitations have stimulated the development of artificial discs that aim to relieve pain whilst preserving physiological motion. Over the last fifty years, there have been many attempts to produce artificial intervertebral discs, but very few of these have reached the stage of in vivo tests, and fewer still have been used in patients [4]. The majority of the clinically available lumbar disc prostheses aim to restore intervertebral height and maintain spinal flexibility, and although they have had some very successful results, they do not preserve the compliance of a natural intervertebral disc. They use hard components such as metals or durable polymers, which are non-shock absorbing and hence may transfer stresses to adjacent levels in a similar way to spinal fusion.

1.2 The *CAdisc-L*

The *CAdisc-L*, designed by Ranier Technology Ltd., is a polycarbonate urethane lumbar intervertebral disc prosthesis manufactured using a novel injection moulding procedure. The design aims to replicate not only the motion

J. H. Gwynne (✉) · R. E. Cameron
Cambridge Centre for Medical Materials, Department of Materials Science and Metallurgy, University of Cambridge, Pembroke Street, Cambridge CB2 3QZ, UK
e-mail: jhg27@cam.ac.uk

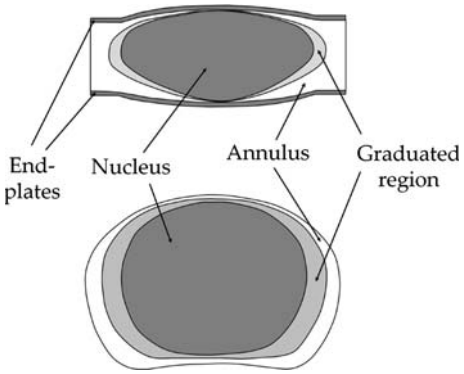

Fig. 1 Vertical (top) and horizontal (bottom) cross-sections through the *CAdisc-L*

but also the axial compliance provided by a natural disc, by mimicking the natural structure as closely as possible. It consists of a lower modulus nucleus surrounded by a higher modulus annulus, with end-plates that will allow both primary and secondary fixation. One of the main advantages of this design is the presence of a graduated modulus region between the annulus and nucleus. A sharp interface between two different materials is likely to be a potential long-term fatigue failure site due to the mismatch in mechanical properties, but any such interfaces have been eliminated from this design and the materials properties change gradually from annulus to nucleus across the disc. Schematic diagrams showing horizontal and vertical cross-sections through the *CAdisc-L* are shown in Fig. 1.

1.3 Polyurethanes [5–7]

The term "polyurethane" refers to a family of polymers with a wide range of properties and applications. They are synthesised by the reaction between an isocyanate, a polyol and often a chain extender, and the mechanical and chemical properties can be varied by changing the ratio of these three. The reaction may be catalysed by a variety of substances, including bases, many metal complexes and acids.

Polyurethanes typically undergo phase separation and exist as a two-phase structure consisting of crystalline hard segments within a matrix of soft segment material. The hard segments are typically formed from the isocyanate (and chain extender, if one is present) and the soft segment contains the polyol. The mechanical properties of the polyurethane, as well as its thermal and hydrolytic stability, are heavily dependent on the hard segment to soft segment ratio.

The biocompatibility of polyurethanes has been well documented in recent years, supported by large quantities of in vivo and in vitro testing [8]. They have been used in a wide variety of applications, including: cardiac valves, wound dressing products, catheters, breast implants, and components in replacement joints.

1.4 Small angle X-ray scattering (SAXS) [9–11]

Any material with a periodic structure can be analysed using X-ray diffraction. The diffraction angle, θ, and the size of the scattering feature, d, are inversely related by Bragg's law:

$$n\lambda = 2d\sin\theta \tag{1}$$

where λ is the wavelength of the X-rays and n is an integer. Whereas wide angle X-ray scattering is traditionally used to provide information about, for example, the distance between crystallographic lattice planes (of the order of a few Å), SAXS is used to study much larger structures, typically with sizes greater than 10 Å. A parameter that is often used in SAXS analysis is the scattering vector, q, which is defined as:

$$q = \frac{4\pi\sin\theta}{\lambda} \tag{2}$$

The intensity measured during a SAXS experiment is related to the electron density and morphology of a sample (and hence the degree of phase separation in a polyurethane) by a Fourier transform. The inverse Fourier transform of the intensity does not, however, lead directly back to the electron density function, which can make the interpretation of SAXS data difficult. Most of the models used to analyse SAXS data for polymers fall into one of the following categories: dilute particulate system, non-particulate two-phase system, soluble blend system and periodic system.

In the dilute particulate system model, particles of one material are dispersed in a uniform matrix of a second. These particles may have a simple geometric shape, such as spheres, thin discs or thin rods (i.e., 3-, 2- and 1-dimensional objects), and the form of the intensity curves at relatively large q (but less than about 1 nm^{-1}), is:

$$I(q) \propto q^{-\alpha} \tag{3}$$

in which the exponent, α, is equal to 4 for spheres, 2 for thin discs and 1 for thin rods. If $ln(I)$ is plotted against $ln(q)$, the gradient will be equal to $-\alpha$.

It is often more useful to consider the scattering behaviour of a random coil configuration than a solid sphere since polymer chains generally do not completely fill the scattering volume. The scattering intensity due to a random coil chain obeying a Gaussian approximation is described by the following equation:

$$I(q) = \rho_0^2 v^2 D(x) \tag{4}$$

where ρ_0 is the scattering density, v is the particle volume and $D(x)$ is the Debye function, which has the form:

$$D(x) = \frac{2(e^x + x - 1)}{x^2} \tag{5}$$

in which: $x = q^2 R_g^2$

R_g is the radius of gyration, which is a measure of the characteristic size of the particle. As q increases, $D(x)$ (and therefore the intensity) varies with q^{-2}, in contrast to the exponent of four obtained for solid spheres. This reflects the more open structure of the Gaussian coil relative to that of a solid sphere and may also be explained in terms of fractals [12] since, as mentioned above, the polymer chain fills only a certain fraction of the scattering volume. The fact that the intensity curves for solid thin discs and for random coil chains have the same gradient (at relatively large q) demonstrates that it may not always be possible to unambiguously interpret SAXS data.

Even when the shape of the particles is unknown or irregular, their radius of gyration may still be determined, since the scattering function is found to follow a universal form, known as the Guinier law, given by:

$$I(q) = \rho_0^2 v^2 \exp(-\frac{1}{3}q^2 R_g^2) \quad (6)$$

This law is valid provided that q is much smaller than $1/R_g$, the system is dilute (so particles scatter independently) and the system is isotropic. If the logarithm of $I(q)$ is plotted against q^2 (known as a Guinier plot), the initial slope gives $-R_g^2/3$, which allows the radius of gyration to be calculated.

A more realistic model for polymer chains than the Gaussian chain model can be obtained by considering a Kratky–Porod chain, in which the rigidity of a polymer molecule is taken into account. At small q, the intensity falls as predicted by the Guinier law. However, as q increases, the curve reflects the random coil nature of the molecule and follows the Debye equation before showing the q^{-1} behaviour of thin rods at large values of q.

The non-particulate two-phase system model describes two different materials which are irregularly intermixed, neither being considered the matrix nor the dispersed phase. Examples include crystalline and amorphous regions in a semi-crystalline polymer, and two immiscible polymers that have been blended. The data may be analysed to determine the state of dispersion of the materials in the sample, including, for example, the characteristic size of the domains.

An ideal two-phase system is one containing only two different phases, which have sharp interfaces with no measurable thickness between them. It is found that $I(q)$ decreases with q^{-4} for large q and that the proportionality constant is related to the total area, S, of the boundaries between the two phases within the scattering volume. This is described by Porod's law, which states that as $q \to \infty$:

$$I(q) \to \frac{2\pi(\Delta\rho_0)^2 S}{q^4} \quad (7)$$

The soluble blend system model describes a single phase material in which two components are dissolved molecularly as a homogeneous solution. Examples include a miscible polymer blend, a dissolved polymer and a block copolymer in a disordered state.

The periodic system category contains ordered structures which have a period of repetition on the order of 1–100 nm, including semicrystalline polymers consisting of stacks of lamellar crystals and ordered block copolymers.

1.5 SAXS of polyurethanes

Although a substantial amount of work has been carried out involving SAXS studies of thermoplastic polyether urethane samples (for a review, see Laity et al. [13]), there is no available literature for the specific polycarbonate urethanes studied during this work, since they are manufactured using novel formulations. Little work has been carried out on polycarbonate urethanes, the closest formulation to those studied here being a non-crosslinked polycarbonate urethane manufactured from polycarbonate diol, 1,4-butane diol and methylene-bis-diphenylisocyanate (MDI), which was found to contain crystalline hard segment domains [14]. However, since small changes to the chemistry of polyurethanes can have a huge effect on their morphology and properties, SAXS results for different formulations are very varied.

1.6 Aims

The primary objective of this work was to develop an analysis method that could be used to establish the variation in composition across the graduated region within prototype *CAdisc-L* samples. The polyurethanes making up the annulus and nucleus materials are chemically very similar, meaning that techniques such as Fourier Transform Infra-Red (FTIR) spectroscopy, Raman spectroscopy and X-ray microtomography do not show a large enough difference across a disc sample to analyse the composition reliably and quantitatively. SAXS was found to be a suitable technique for distinguishing the two materials, but it will be shown that it was necessary to formulate an empirical analysis method. This method can be applied to any polymeric system in which there is a systematic variation in SAXS response with composition.

2 Materials and methods

2.1 Materials

The polyurethanes making up the annulus and nucleus materials are manufactured from the same chemical components, but these are present in different relative

proportions, which gives the two materials different mechanical properties. These components are:

- Methylene-bis-(4-cyclohexylisocyanate), or HMDI, which forms the hard segment material
- Polycarbonate diol, which forms the soft segment material
- Glycerol, which is trifunctional and acts as a cross-linker
- METATIN^{TM} catalyst 812 ES, which is a tin-based catalyst

HMDI exists as a mixture of diastereoisomers [5], which has been found to inhibit crystallisation. As a result, polyurethanes formed from HMDI typically contain many small amorphous or semi-crystalline domains within the soft segment matrix, rather than undergoing phase separation in the traditional sense to form discrete crystalline hard segments [15].

The proportion of glycerol, and therefore the degree of crosslinking, is higher in the annulus material than in the nucleus material.

The polyurethanes are formed using a prepolymer method, each polyurethane being produced from two prepolymers, which are mixed just before injection into the mould. During the manufacturing process, the pure annulus material is injected into the disc mould first, followed by the material making up the graduated region, followed by the pure nucleus material. This is achieved in one single moulding step, so little curing takes place until after moulding is finished. The graduated region is manufactured using a series of moulding increments, the proportion of annulus material decreasing and the proportion of nucleus material increasing between successive increments. Each increment has the same volume, but the volume can be varied between samples to produce different graduated regions. After injection of the polymers into the moulds, they are placed in a pressure pot (pressurised to 60 psi to prevent the formation of bubbles during curing) and put into an oven at 80°C overnight to complete the curing process.

2.2 Samples

1. Calibration samples ranging in composition from pure annulus material to pure nucleus material in 10% increments (i.e. 100% annulus, 90% annulus/10% nucleus, 80% annulus/20% nucleus, etc.). These were manufactured as 5 mm thick sheets.
2. Prototype *CAdisc-L* samples with graduated regions ranging between 0 and 50% of the total disc volume.
3. An "insert moulded" sample: unlike in the prototype *CAdisc-L* samples, in this sample the injection moulded nucleus was allowed to cure fully before subsequent moulding of the surrounding annulus material, in order to achieve as sharp an interface between these two regions as possible.

All samples used for SAXS analysis were 1 mm thick. This thickness was chosen such that the disc samples would be thin enough for there to be no significant change in composition through the thickness of the sections, but thick enough to be able to be cut accurately and reproducibly. The calibration and disc samples were sectioned using a Struers Accutom circular saw with a blade specifically designed for the cutting of polymers. Sections were cut laterally from the centres of disc sections, since this was the direction in which the graduated region was widest, so the effect of changing its volume would be most noticeable.

2.3 SAXS

SAXS experiments were carried out on a Bruker NanoSTAR. A collimated beam of Cu-Kα X-rays was used and the scattered X-rays were collected by a 2D detector. A sample-to-detector distance of 26 cm was used, allowing data collection over the 2θ range of 0.4–11.0°.

Samples were mounted on a holder which fits into a moveable stage within the NanoSTAR. The horizontal and vertical coordinates of the stage are computer-controlled, meaning that the X-ray beam could be directed accurately through any chosen part of the sample.

2.3.1 Background correction

In order to carry out a background correction, data was collected with no sample in place between the X-ray beam and the detector for the same amount of time for which sample data was collected. Since the background radiation measured during sample data acquisition is proportional to the quantity of X-rays that pass through the sample, it was not possible to simply subtract the background data from the sample data. Instead, the sample transmission needed to be taken into account. This was calculated using a sample of glassy carbon, which is a material with a very high scattering intensity. This is present in the NanoSTAR on a rotating sample wheel which allows it to be rotated into the path of the X-ray beam.

The background correction was calculated using the following formula [16]:

$$I_{corr} = I_x - \tau_x I_0 \tag{8}$$

where I_{corr} is the corrected sample scattering intensity, I_x is the uncorrected sample scattering intensity, τ_x is the sample transmission and I_0 is the background intensity.

The sample transmission, τ_x, was calculated using the formula [16]:

$$\tau_x = \frac{I_{x+GC} - \tau_{GC} I_x}{I_{GC} - \tau_{GC} I_0} \quad (9)$$

where I_{x+GC} is the intensity measured when the X-ray beam passes through both the glassy carbon and the sample, I_{GC} is the glassy carbon sample intensity, and τ_{GC} is the glassy carbon sample transmission (which has a value of 0.16).

Due to the very high scattering intensity of the glassy carbon sample, I_{x+GC} and I_{GC} could be collected for a much shorter time than the sample and background data. For this work, I_{x+GC} and I_{GC} were collected for 50 s, whereas the sample and background data needed to be collected for 10,000 s, since these polyurethanes do not scatter X-rays very strongly.

2.3.2 Data analysis

As will be seen in Sect. 3.2, the two-dimensional data collected by the NanoSTAR detector were circularly symmetric for all the samples studied during this work, indicating that the materials were isotropic. This allowed the data to be analysed using an azimuthal integration to provide a one-dimensional variation of intensity with 2θ in the range 0.4–11.0°. This was carried out using the NanoSTAR software and a data interval of 0.01° was employed. The data were imported into Microsoft Excel and the background corrections were carried out, as described above. The data were also smoothed over five data points to decrease noise.

2.3.3 Beam width

Since the X-ray beam is not infinitely narrow, the width of the beam introduces an error into the measurement of the composition at any particular position when carrying out the linescans described below.

To measure the width of the X-ray beam (and hence obtain an estimate of the error), an empty aluminium sample holder was placed inside the sample chamber and the glassy carbon sample was rotated into place. The sample holder was positioned such that the entire X-ray beam was directed into the side of holder itself. A series of 30 s scans was carried out, the stage being moved horizontally in 0.025 mm increments between each scan. As the stage moved, the X-ray beam gradually emerged from behind the sample holder until it was fully exposed, and the intensity increased from zero to a maximum value.

2.3.4 Calibration samples

In order to produce a calibration curve to quantify the variation of SAXS behaviour with composition, the 1 mm thick calibration samples were mounted on the aluminium sample holder and scans were carried out on each sample.

2.3.5 CAdisc-L samples

To ascertain the variation in composition across discs with differing graduated regions, the 1 mm thick lateral sections were mounted on the sample holder. This was positioned such that the X-ray beam would pass through the pure annulus material 1 mm from the edge of the disc section, at a height corresponding to the widest part of the nucleus region. A series of scans was carried out, the stage being moved horizontally in 0.4 mm increments between each scan, such that data were acquired from the pure annulus material, across the graduated region and into the pure nucleus material. This is illustrated schematically in Fig. 2, in which the nucleus material has been dyed to highlight its position (although it should be noted that the dotted line is not an accurate representation of the X-ray beam width or the distance between scans).

3 Results

3.1 Beam width

A graph showing intensity against the distance moved by the stage is shown in Fig. 3a. It can be seen that the distance over which the intensity increases is given by approximately 0.8 mm, which gives a good estimate of the total width of the X-ray beam.

However, since the intensity of the beam decreases with distance from its centre, a more useful parameter is the full width at half maximum (FWHM) of the beam profile. The FWHM is commonly used to describe the width of a curve and is given by the distance between points on the curve at which the function reaches half its maximum height. To obtain the beam profile, the differential of the curve in Fig. 1a was calculated (since the change in total intensity at each increment will be the intensity due to the newly

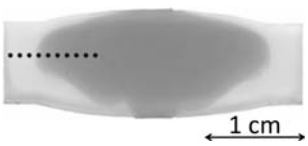

Fig. 2 1 mm disc section showing locations of SAXS scans

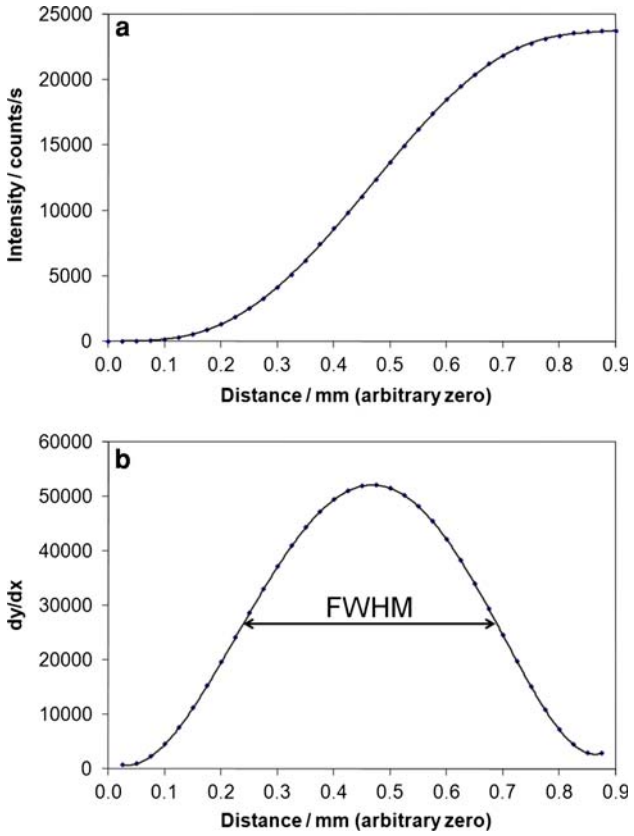

Fig. 3 Intensity against distance (**a**), and beam profile showing FWHM (**b**)

exposed part of the beam). The beam profile is shown in Fig. 3b and the FWHM was measured to be 0.45 mm.

3.2 Calibration samples

2D diffraction patterns for the annulus and nucleus materials are shown in Fig. 4. These are circularly symmetric, which shows that the materials are isotropic, and it can be seen that the main difference between the two materials is the presence of a bright patch at very low angles for the

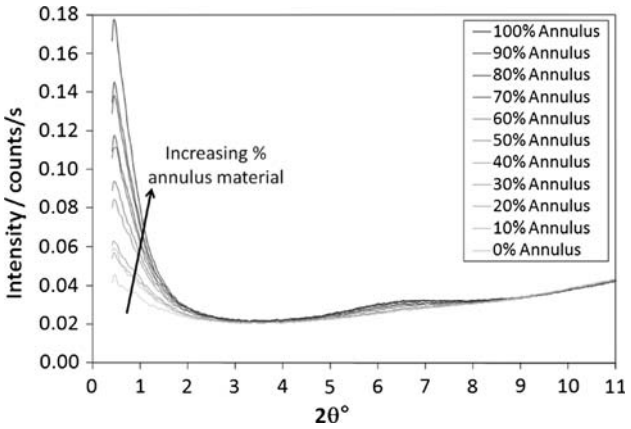

Fig. 5 SAXS response of calibration samples

annulus material, which corresponds to a higher intensity. It should be noted that the dark circle at the centres of the images corresponding to a region of zero intensity is due to the presence of a beam stop: this prevents damage from occurring to the detector by blocking the straight-through beam.

Figure 5 shows intensity against $2\theta°$ for all the calibration samples, and it can be seen that the intensity at very low angles decreases systematically as the composition changes from annulus to nucleus. A small broad peak is also present from approximately $2\theta = 5°$ to $2\theta = 8°$ in the annulus material (corresponding to d values of approximately 11–18 Å), but this decreases in intensity as the composition becomes more nucleus-rich and is not observed at all in the pure nucleus material. It is not clear to what this peak corresponds, but it is thought to be related to the fact that the annulus material contains a higher density of crosslinks.

The SAXS data for these polyurethanes were found to be difficult to interpret and no definite conclusions could be drawn using the conventional data analysis methods described previously. Figure 6a shows intensity, I, against q for the annulus and nucleus materials and Fig. 6b shows $ln(I)$ against $ln(q)$. In the region between $ln(q) = -0.7$ and

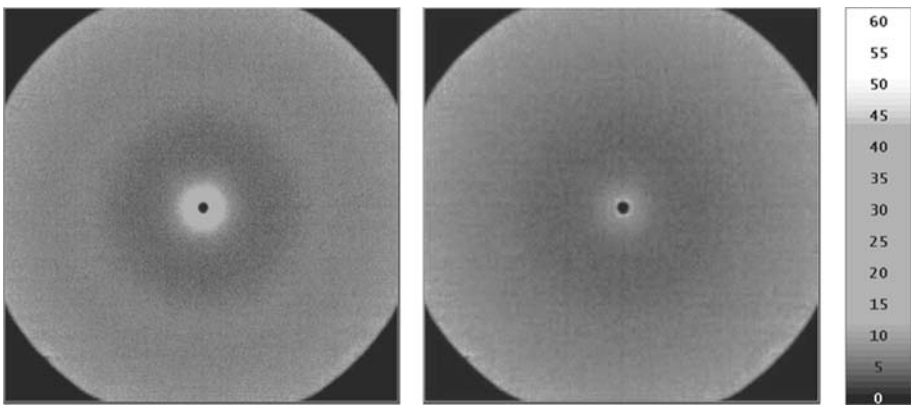

Fig. 4 2D diffraction patterns for annulus (left) and nucleus (right) material (the scale bar shows intensity in counts)

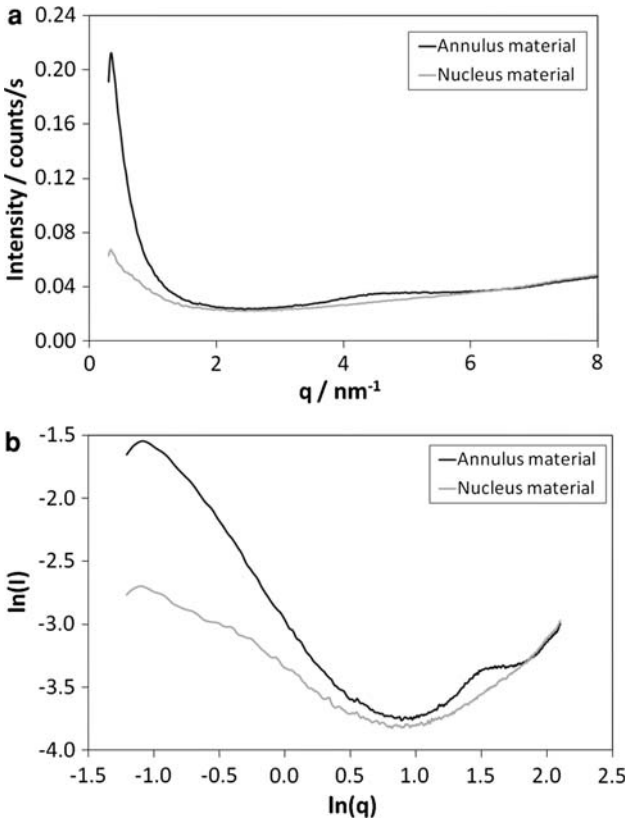

Fig. 6 I vs. q (top) and $ln(I)$ vs. $ln(q)$ (bottom) for the annulus and nucleus materials

$ln(q) = 0.2$, the annulus curve has a gradient of -1.5 and the nucleus curve has a gradient of -0.7. These values, particularly that for the nucleus material, do not appear to fit any of the models well. A gradient of -1.5 would fall halfway between that expected for a 1D scattering object and a 2D one (or a random coil), but a gradient of -0.7 is meaningless, which may suggest that there are no distinct interfaces between scattering bodies.

It is also impossible to calculate an estimate of the radius of gyration for the two materials, since these data do not include low enough values of q to be reliably within the Guinier range.

In order to quantify the variation in SAXS response with composition, an intensity ratio was established, since the absolute intensity values depended on a number of factors such as the age of the X-ray source. Slight variations in sample thickness could also produce slightly different absolute intensities.

The intensity ratio chosen was the ratio of the intensity at $2\theta = 0.8°$ (which is a region of the graph where the intensity depends strongly on composition) to the intensity at $2\theta = 3.5°$ (where the intensity is much more constant between different samples). A graph showing the variation of the intensity ratio with composition is shown in Fig. 7.

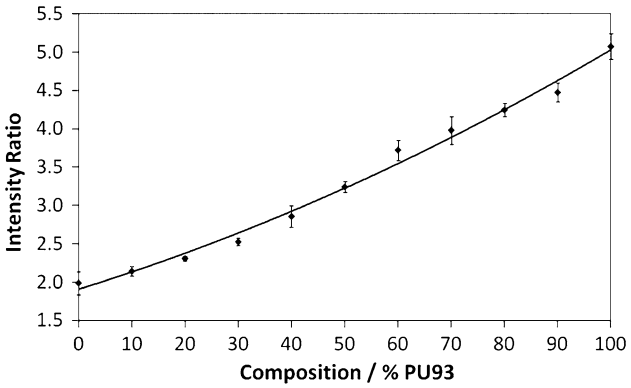

Fig. 7 SAXS calibration curve

A quadratic line has been fitted to the data, since this was found to fit the end-points better than a straight line. This curve was used to calibrate the subsequent SAXS data.

3.3 Linescans

Intensity against 2θ graphs are shown in Fig. 8 for insert moulded and 40% graduated samples, all the lines for each

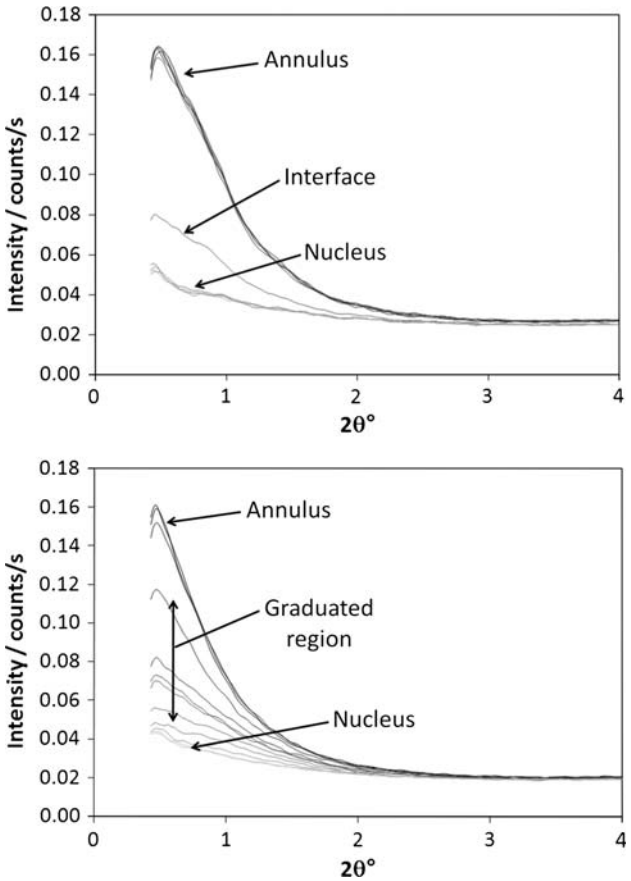

Fig. 8 SAXS data for insert moulded (top) and 40% graduated (bottom) samples

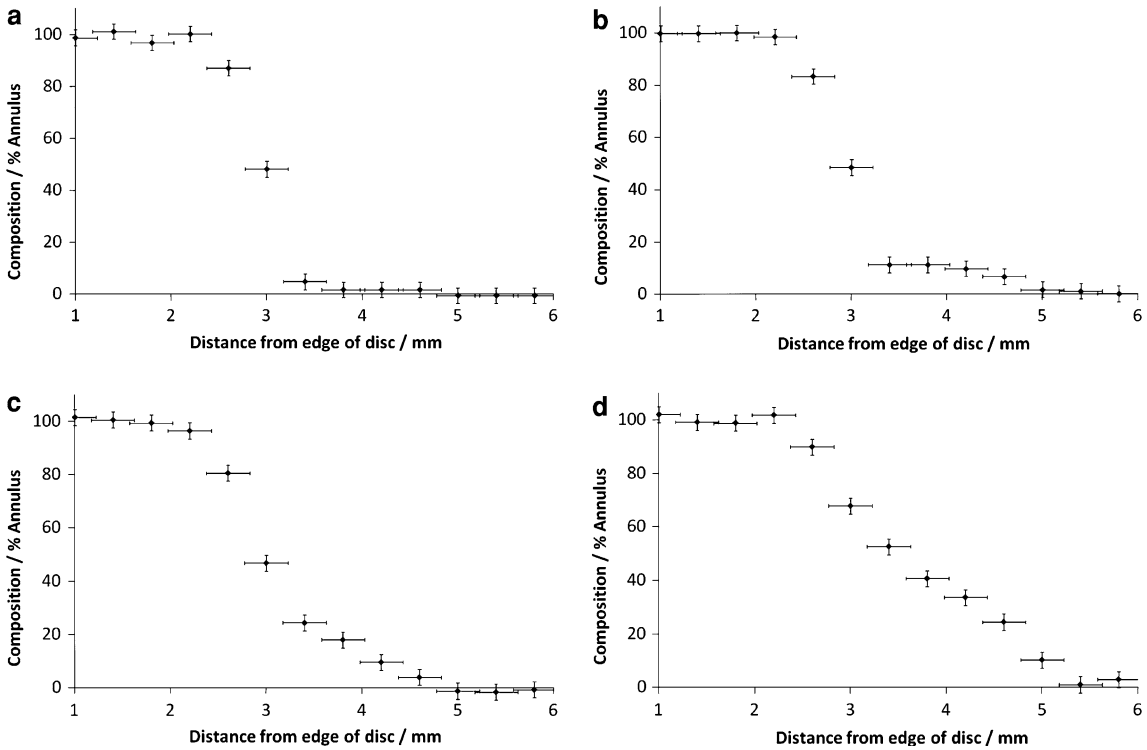

Fig. 9 Graphs showing the variation in composition with distance across insert moulded (**a**), 0% graduated (**b**), 20% graduated (**c**) and 50% graduated (**d**) samples

linescan being plotted on the same graph. Data are only shown in the range 0–4°, since this includes both values needed to calculate the intensity ratio. The main difference between these graphs is the number of lines separating the scans corresponding to pure annulus and pure nucleus material. The insert moulded sample only shows one line between the two extremes, corresponding to a sharp interface, whereas the 40% graduated sample shows several more, corresponding to a much wider interface.

The intensity ratio established earlier was calculated for each line in each linescan and related to composition using the calibration graph, allowing the variation in composition with distance across the samples to be determined. Composition against distance graphs for a variety of samples are shown below, in Fig. 9. The horizontal error bars, representing the error in position, correspond to the FWHM of the X-ray beam and the vertical error bars, representing the error in the composition, correspond to the average deviation in composition of points in the calibration curve from the line of best fit (approximately 3%).

4 Discussion

As described above, although the SAXS data do not easily fit any of the standard analysis models, there is a systematic variation in intensity ratio which can be used to quantify the change in SAXS response with composition. One explanation for the difference in scattering behaviour between the annulus and nucleus materials is that it may be caused by the higher amount of crosslinking in the annulus material than the nucleus material. During polymerisation, alcohol groups (on the polycarbonate diol or the glycerol) can only react with isocyanate groups in HMDI molecules, which each contain two bulky six-membered rings. The reaction of glycerol with the isocyanate therefore results in six of these bulky groups being in relatively close proximity and forming a "cluster". These clusters may act as scattering features, so higher concentrations of glycerol will result in higher concentrations of clusters, producing a higher SAXS intensity.

For all prototype *CAdisc-L* samples, the intensity ratios for the annulus regions consistently gave a composition of 100% annulus materials (within the height of the error bars), and those for the nucleus regions also corresponded to a composition of 0% annulus material (i.e., 100% nucleus material). This indicates that this method of calibrating the variation in SAXS behaviour with composition gives reasonably reliable results.

It can be seen that the sharpest interface occurs in the insert moulded sample, as expected. The interface in the 0% graduated sample is not as sharp as this because some interdiffusion of the molecules can occur across the interface: polymerisation only begins when the prepolymers are

mixed just before injection into the mould, so the annulus and nucleus materials are still largely unpolymerised and are able to diffuse to some extent. The width of the graduated region increases as its volume increases, ranging from less than 1 mm in the 0% graduated sample to over 3 mm in the 50% graduated sample.

The composition does not vary linearly across the graduated region, the change being sharpest closest to the annulus region. One possible explanation can be obtained by considering the injection moulding of the graduated region: each increment has the same volume, but the increments closest to the annulus are spread over larger areas than those closest to the nucleus (since the surface area of the outside of the nucleus region is smaller than the surface area of the inside of the annulus region), so the increments are effectively thinner closer to the annulus, making the change in composition sharper. The composition profile is further blurred by interdiffusion of the polymer molecules.

5 Conclusions

This work has shown that Small Angle X-ray Scattering is a useful technique for studying the variation in chemical properties across a graduated region, even when the data do not fit the standard analysis models. Linescans have shown that the graduated regions in these prototype disc samples range from less than 1 mm to over 3 mm in width, and also that the composition does not vary linearly across the graduated region, the change being sharpest closest to the annulus region. The presence of a graduated region between the annulus and nucleus is likely to be beneficial to the lifetime and performance of the device, since it eliminates sharp interfaces between materials with different mechanical properties and instead allows the properties to change gradually across the disc.

Although this work concerns one specific series of polyurethanes, the method used here could be adapted for a wide variety of polymer formulations: as long as a difference in SAXS behaviour can be seen between the two composition end-points, an intensity ratio can be chosen such that it varies strongly with composition and a calibration curve can be produced in order to reliably estimate the composition of any unknown sample.

Acknowledgements The authors would like to acknowledge Dr Peter Laity for helpful discussions about polyurethanes and SAXS, and Dr Scott Johnson and Steven Scott at Ranier for guidance and help with sample manufacture respectively. Funding for this research was gratefully received from the EPSRC and Ranier Technology Ltd.

References

1. Bogduk N. Clinical anatomy of the lumbar spine and sacrum. 3rd ed. Edinburgh: Churchill Livingstone; 1997.
2. An H, Boden SD, Kang J, Sandhu HS, Abdu W, Weinstein J. Summary statement—emerging techniques for treatment of degenerative lumbar disc disease. Spine. 2003;28:S24–5.
3. Boden SD, Balderston RA, Heller JG, Hanley EN, Zigler JE. An AOA critical issue—disc replacements: this time will we really cure low-back and neck pain? J Bone Jt Surg. 2004;86A:411–22.
4. Szpalski M, Gunzburg R, Mayer M. Spine arthroplasty: a historical review. Eur Spine J. 2002;11:S65–84.
5. Szycher M. Szycher's handbook of polyurethanes. Boca Raton: CRC Press; 1999.
6. Woods G. The ICI polyurethanes book. 2nd ed. New York: ICI Polyurethanes and John Wiley & Sons; 1990.
7. Lamba NMK, Woodhouse KA, Cooper SL. Polyurethanes in biomedical applications. Boca Raton: CRC Press LLC; 1998.
8. Vermette P, Levesque S, Griesser HJ. Biomedical applications of polyurethanes. TX: Landes Bioscience; 2001.
9. Roe R-J. Methods of X-ray and neutron scattering in polymer science. New York: Oxford University Press; 2000.
10. Glatter O, Kratky O. Small angle x-ray scattering. London: Academic Press; 1982.
11. Guinier A. X-ray diffraction in crystals, imperfect crystals and amorphous bodies. San Francisco: W.H. Freeman; 1963.
12. Schmidt P. Small-angle scattering studies of disordered, porous and fractal systems. J Appl Crystallograph. 1991;24:414–35.
13. Laity PR, Taylor JE, Wong SS, Khunkamchoo P, Norris K, Cable M, et al. A review of small-angle scattering models for random segmented poly(ether-urethane) copolymers. Polymer. 2004;45:7273–91.
14. Guo J, Zhao M, Ti Y. Study on structure and performance of polycarbonate urethane synthesized via different copolymerization methods. J Mater Sci. 2007;42:5508–15.
15. Van Bogart JWC, Lilaonitkul A, Lerner LE, Cooper SL. Morphology and properties of short segment block copolymers. J Macromolecular Sci Phys. 1980;B17:267–301.
16. NanoSTAR SAXS System: User's Manual. Vol. 2. Bruker SAXS; 2003.